



# Material properties of tapered crystalline silicon core fibers

Y. FRANZ,<sup>1</sup> A. F. J. RUNGE,<sup>1</sup> H. REN,<sup>1</sup> N. HEALY,<sup>2</sup> K. IGNATYEV,<sup>3</sup>  
M. JONES,<sup>4</sup> T. HAWKINS,<sup>4</sup> J. BALLATO,<sup>4</sup> U. J. GIBSON,<sup>5</sup> AND  
A. C. PEACOCK<sup>1,\*</sup>

<sup>1</sup>Optoelectronics Research Centre, University of Southampton, SO17 1BJ, UK

<sup>2</sup>Emerging Technology and Materials Group, Newcastle University, NE1 7RU, UK

<sup>3</sup>Diamond Light Source Ltd, Harwell Science and Innovation Campus, Didcot, OX11 0DE, UK

<sup>4</sup>Department of Materials Science and Engineering, Clemson University, Clemson, SC 29634, USA

<sup>5</sup>Department of Physics, Norwegian University of Science and Technology, 7491 Trondheim, Norway

\*[acp@orc.soton.ac.uk](mailto:acp@orc.soton.ac.uk)

**Abstract:** Crystalline silicon optical fibers are emerging as a promising platform for a wide range of optoelectronic applications. Here we report a crystallographic study of the material properties within silicon fibers that have been post-processed via a tapering procedure to obtain small, few micron-sized core diameters. Our results reveal that the tapering process can improve the polysilicon quality of the core through the formation of large, centimeter long crystal grains, thus significantly reducing the optical losses.

Published by The Optical Society under the terms of the [Creative Commons Attribution 4.0 License](#). Further distribution of this work must maintain attribution to the author(s) and the published article's title, journal citation, and DOI.

**OCIS codes:** (060.2280) Fiber design and fabrication; (160.6000) Semiconductor materials.

## References and links

1. A. C. Peacock, U. J. Gibson, and J. Ballato, "Silicon optical fibers - past, present, and future," *Appl. Phys. X* **1**, 114 (2016).
2. R. He, P. J. A. Sazio, A. C. Peacock, N. Healy, J. R. Sparks, M. Krishnamurthi, V. Gopalan, and J. V. Badding, "Integration of gigahertz-bandwidth semiconductor devices inside microstructured optical fibers," *Nat. Photonics* **6**, 174 (2012).
3. F. A. Martinsen, B. K. Smeltzer, M. Nord, T. Hawkins, J. Ballato, and U. J. Gibson, "Silicon-core glass fibers as microwire radial-junction solar cells," *Sci. Rep.* **4**, 6283 (2014).
4. F. H. Suhailin, L. Shen, N. Healy, L. Xiao, M. Jones, T. Hawkins, J. Ballato, U. J. Gibson, and A. C. Peacock, "Tapered polysilicon core fibers for nonlinear photonics," *Opt. Lett.* **41**, 1360 (2016).
5. J. R. Sparks, R. He, N. Healy, M. Krishnamurthi, A. C. Peacock, P. J. A. Sazio, V. Gopalan, and J. V. Badding, "Zinc Selenide Optical Fibers," *Adv. Mater.* **23**, 1647 (2011).
6. L. Lagonigro, N. Healy, J. R. Sparks, N. F. Baril, P. J. A. Sazio, J. V. Badding, and A. C. Peacock, "Low loss silicon fibers for photonics applications," *Appl. Phys. Lett.* **96**, 041105 (2010).
7. J. Ballato, T. Hawkins, P. Foy, R. Stolen, B. Kokuoz, M. Ellison, C. McMillen, J. Reppert, A. M. Rao, M. Daw, S. Sharma, R. Shori, O. Stafsudd, R. R. Rice, and D. R. Powers, "Silicon optical fiber," *Opt. Express* **16**, 18675 (2008).
8. E. F. Nordstrand, A. N. Dibbs, A. J. Eräker, and U. J. Gibson, "Alkaline oxide interface modifiers for silicon fiber production," *Opt. Mater. Express* **3**, 651 (2013).
9. C. McMillen, G. Brambilla, S. Morris, T. Hawkins, P. Foy, N. Broderick, E. Koukharenko, R. Rice, and J. Ballato, "On crystallographic orientation in crystal core optical fibers II: Effects of tapering," *Opt. Mat.* **35**, 93 (2012).
10. J. S. Orcutt, S. D. Tang, S. Kramer, K. Mehta, H. Li, V. Stojanović, and R. J. Ram, "Low-loss polysilicon waveguides fabricated in an emulated high-volume electronics process," *Opt. Express* **20**, 7243 (2012).
11. D. Kwong, J. Covey, A. Hosseini, Y. Zhang, X. Xu, and R. T. Chen, "Ultralow-loss polycrystalline silicon waveguides and high uniformity 1x12 MMI fanout for 3D photonic integration," *Opt. Express* **20**, 21722 (2012).
12. S. Shabahang, J. J. Kaufman, D. S. Deng, and A. F. Abouraddy, "Observation of the Plateau-Rayleigh capillary instability in multi-material optical fibers," *Appl. Phys. Lett.* **99**, 161909 (2011).
13. R. Wang, G. Zhou, Y. Liu, S. Pan, H. Zhang, D. Yu, and Z. Zhang, "Raman spectral study of silicon nanowires: High-order scattering and phonon confinement effects," *Phys. Rev. B* **61**, 827 (2000).
14. N. Healy, M. Fokine, Y. Franz, T. Hawkins, M. Jones, J. Ballato, A. C. Peacock, and U. J. Gibson, "CO<sub>2</sub> laser-induced directional recrystallization to produce single crystal silicon-core optical fibers with low loss," *Adv. Opt.*

- Mater. **4**, 1004 (2016).
15. N. Healy, J. R. Sparks, P. J. A. Sazio, J. V. Badding, and A. C. Peacock, "Tapered silicon optical fibers," Opt. Express **18**, 7596 (2010).
16. B. Scott and G. Pickrell, "Silicon optical fiber diameter dependent grain size," J. Cryst. Growth **371**, 134 (2013).
17. A. C. Peacock, "Soliton propagation in tapered silicon core fibers," Opt. Lett. **35**, 3697 (2010).
18. N. Healy, S. Mailis, N. M. Bulgakova, P. J. A. Sazio, T. D. Day, J. R. Sparks, H. Y. Cheng, J. V. Badding, and A. C. Peacock, "Extreme electronic bandgap modification in laser-crystallized silicon optical fibers," Nat. Materials **13**, 1122 (2014).

## 1. Introduction

Semiconductor optical fibers with crystalline core materials are currently experiencing growing popularity amongst the novel material fiber community [1]. Compared to their glass-based counterparts, these fibers offer a number of advantageous properties, such as rich optoelectronic functionality and high damage thresholds, that are of use for the development of photodetectors [2], solar-cells [3], nonlinear optical components [4], as well as infrared delivery systems and lasers [5]. Currently there are two main approaches to fabricating these fibers, the first makes use of a chemical deposition method [6] and the second is based on a derivative of the more conventional fiber drawing approach [7]. Of these methods, it is the latter technique that has been the most widely adopted by the community, principally as it is fast and capable of producing long lengths of fiber with a uniform cross-section. However, a significant draw-back of this approach is that, owing to the high drawing temperatures required to melt the semiconductor core, it can be difficult to produce continuous lengths of fiber with high optical quality cores that have the micron-sized dimensions required for many optoelectronics applications [7, 8].

Starting from the as-drawn crystalline silicon fibers, we have recently developed a modified tapering procedure that allows for the scaling down of the cores to diameters of a micrometer, or less [4]. Importantly, this post-processing method has been shown to further improve the optical quality of the polysilicon core material [9], with the optical losses reducing from 12 dB/cm in the 10  $\mu\text{m}$  diameter as-drawn fibers, down to 3.5 dB/cm in a 1  $\mu\text{m}$  tapered core [10, 11]. To the best of our knowledge, this loss value is the lowest reported for a polysilicon waveguide with core dimensions on the order of  $\sim 1 \mu\text{m}$  and, as a result, these tapered silicon fibers have enabled the first observation of nonlinear propagation in this material. However, clearly, reducing the losses even further would greatly improve the practicality of these fibers, motivating a detailed study of the material properties in the tapered cores.

In this paper, we investigate a range of tapered silicon optical fibers, fabricated to have varying core dimensions, and report the first characterization of the crystallographic properties of their re-processed core material. Micro-Raman spectroscopy, X-ray diffraction (XRD), and optical loss measurements are used to assess the quality of the crystalline silicon core material, before and after tapering, to gain insight into the recrystallization process. Our results show that the act of tapering increases the crystal grain size from a few millimeters, up to almost a centimeter in length, greatly reducing the defect material in the core, which can cause additional absorption and scattering. Optimization of this process has produced fibers with losses as low as 2 dB/cm for core sizes in the range 1-2  $\mu\text{m}$ . Finally, the ultra-smooth nature of the high index contrast silicon/silica interface is confirmed via scanning electron microscopy (SEM) and surface profiling, indicating that the tapering method should be suitable for the production of high optical quality silicon core fibers with nanometer-sized dimensions.

## 2. Fabrication of tapered silicon fibers

The polysilicon fibers studied in this work were fabricated following a two step process. Firstly, fibers with a crystalline silicon core material were fabricated using the molten core drawing technique described in [8]. Briefly, a rod of pure silicon was sleeved inside a silica cladding that

was coated with a thin layer of calcium oxide (CaO). This interface layer is critical as it acts as a stress buffer and also prevents oxygen in-diffusing from the cladding to the core during the high temperature draw process. A standard drawing tower was then used to draw the preform into a fiber, where the soft cladding acts as a crucible to contain the molten core. The final fabricated fiber had an outer diameter of OD  $\sim 130\ \mu\text{m}$  and an inner core diameter of ID  $\sim 10\ \mu\text{m}$ , which was polycrystalline in nature [8]. For advanced optical applications, smaller core sizes are highly desirable, but as of to date, Rayleigh-Plateau instability has limited the diameters directly achievable with this technique [12]. To overcome this limitation, we employ a second processing step whereby the as-drawn fibers are tapered down to few micrometer core sizes.

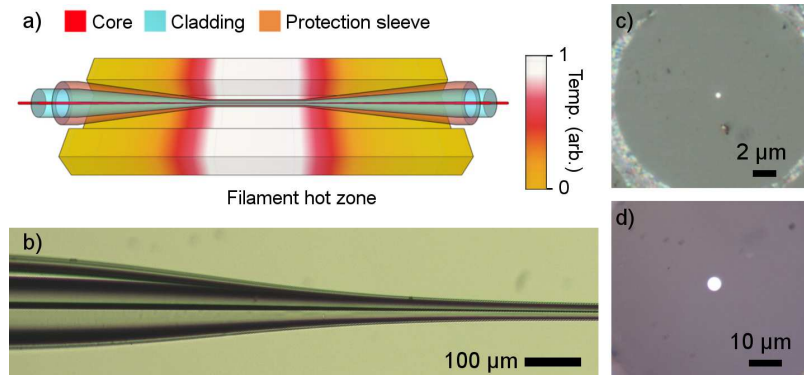


Fig. 1. a) Schematic of the tapering process. b) Longitudinal image of a silicon core tapered fiber. c) & d) Polished fiber cross-sections, with core diameters of  $0.6\ \mu\text{m}$  and  $4.5\ \mu\text{m}$ .

A Vytran tapering rig (GPX-3300) was used in this work and was set in the static hot-zone configuration. The hot-zone has a profile that is cooler at the edges, as illustrated in Fig. 1(a), to ensure continuity of the taper transitions at their extremities. The as-drawn fiber is first encased in a thick silica capillary, which helps to strengthen the structure as it is tapered to smaller dimensions. The sleeved fiber is then placed in the tapering rig, where it is heated by a tungsten filament while two motors pull the ends of the fiber apart. During the process, both the silica cladding and the silica sleeve are softened and fuse, while the melted silicon core reshapes and recrystallizes as it cools down. The tapered fibers fabricated via this technique display a smooth transition from the untapered fiber down to the waist, as seen in Fig. 1(b). By adjusting the filament power between 52-59 W, and the pulling velocity between 0.4-0.45 mm/s, a range of tapering ratios have been obtained, from 1:2 to 1:20, demonstrating the versatility of this process [4]. To illustrate this, Fig. 1 also shows microscope images of the cross-section of two tapered fiber core waists, where (c) has a diameter of  $0.6\ \mu\text{m}$  and (d)  $4.5\ \mu\text{m}$ .

### 3. Raman spectroscopy analysis

An initial assessment of the material properties of the tapered silicon cores was achieved by taking a series of micro-Raman spectra along the fiber, from the untapered fiber down to the waist region. The measurements were performed with a 532 nm laser, which was focused onto the silicon core through the silica cladding. The backscattered Raman signal was recorded on a CCD detector. In order to deconvolve the Lorentzian response of the material from the Gaussian instrument broadening, a Voigt function was used to fit the experimental data. The fiber used in the measurements had a core waist that was  $2\ \mu\text{m}$  in diameter, and the variations in the Lorentzian peak width and position along the length are plotted in Fig. 2(a) and (b), respectively.

From the results in Fig. 2(a) we see that the peak width  $\Gamma$  is largely unaffected by the tapering process, within the resolution of our system, with all three sections exhibiting an average value

of  $\Gamma=3.04\pm 0.08\text{ cm}^{-1}$ . This is slightly larger than the width of our single crystal silicon reference ( $\Gamma=2.7\text{ cm}^{-1}$ ), which suggests that the core maintains a polycrystalline form during the processing. On the other hand, the position of the peak is clearly influenced by the processing, moving further away from the position of the reference peak at  $520\text{ cm}^{-1}$  as the core diameter is decreased. The red shift in the peak position is most likely due to increased stress in the tapered silicon core material, which arises due to the differences in the thermal expansion coefficients of the strongly bonded materials as they cool down [6]. However, it is well known that stress-induced deformation of the silicon lattice can lift the degeneracy of the optical phonon modes, which can manifest as a broadening of the Raman peak [13]. Thus, in order to fully resolve the roles of crystallinity and stress on the tapered core materials, further investigations were undertaken using XRD.

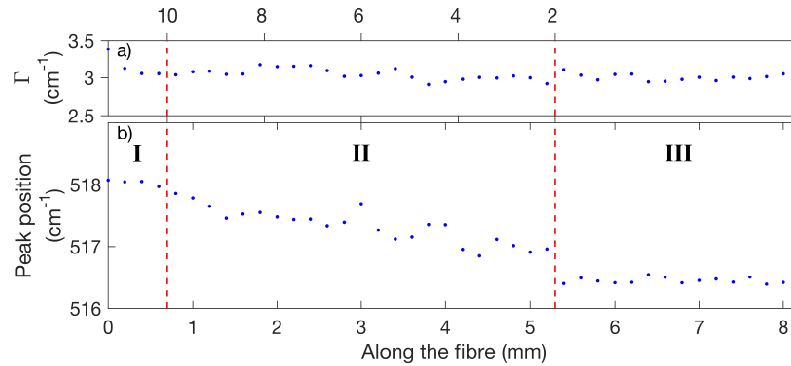


Fig. 2. Evolution of the Raman peak width a) and position b) along a  $2\text{ }\mu\text{m}$  core fiber. The untapered, transition and tapered regions are indicated by I, II and III respectively. The red dashed lines mark out the different sections of the taper.

#### 4. Crystallographic characterization

Owing to the small material volume in the silicon micron-sized fiber cores, the XRD measurements were conducted using a high-energy, micro-focused X-ray beam generated by a synchrotron light source. A schematic of the XRD experimental geometry is shown in Fig. 3(a), where the beam (with a wavelength of  $0.738\text{ }\text{\AA}$ ) is focused through the fiber core from the side, with the diffracted beams being recorded on a CMOS detector placed at the rear. As with the Raman measurements, we measured the Bragg-diffracted X-rays at different positions along the fiber length. Figs. 3(b) and (c) show representative diffraction patterns measured for the as-drawn fiber and the tapered waist, respectively. We note that the stronger signal measured for the as-drawn fiber is simply due to the larger material volume in this section.

It is clear from Fig. 3(b) that there is only one diffraction spot in the detection plane, indicating that the core consists of a single crystal grain which extends across the entire  $10\text{ }\mu\text{m}$  diameter, at least within the width of the X-ray beam ( $\sim 4\text{ }\mu\text{m}$ ). Furthermore, the symmetry of the spot, and the fact that it is well aligned to the reference for the  $\langle 311 \rangle$  crystallographic plane, provides evidence that any residual stress remaining in the core following the high temperature draw process is small. In contrast, the single diffraction spot in Fig. 3(c) is not only asymmetric, elongated perpendicular to the Debye cone, but it is also shifted from the reference position of the closest crystallographic plane, which is  $\langle 220 \rangle$  in this instance. The shift in the spot position arises due to hydrostatic stress induced by the tapering, which corresponds to a reduction in the interlayer spacing from  $1.920\text{ }\text{\AA}$  for the  $\langle 220 \rangle$  plane of bulk silicon to  $1.918\text{ }\text{\AA}$  in our fiber core, and it is this strain that causes the red shift in the Raman peak. Thus the Raman measurements provide a convenient means to track the hydrostatic stress in the core, which clearly increases as the diameter decreases. The stretching of the diffraction spot is then attributed to a component

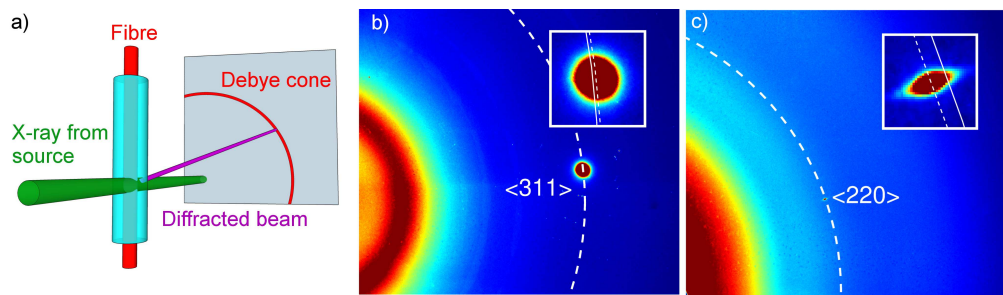


Fig. 3. a) Schematic of the XRD geometry. XRD patterns for single crystal grains sampled within b) the as-drawn fiber and c) the tapered waist section. Large dashed curves indicate the projection of the Debye cone for the silicon planes b)  $\langle 311 \rangle$  and c)  $\langle 220 \rangle$ . Insets show close ups of the diffracted beam, where the dotted curve is aligned to the beam center.

of anisotropic strain, which can manifest as a broadening of the Raman peak. Thus, as the XRD results show that both the as-drawn fiber and the tapered sections have better core crystallinity than the Raman peak width suggests, it is likely that the broad widths reported in Fig. 2(a) are due to some asymmetry in the stress profile.

To test this hypothesis, the X-ray beam was then scanned along the fiber length to map the crystal grain size. The complete mapping of the crystallinity within two  $\sim 1$  cm long sections of the fiber, corresponding to the as-draw fiber (blue diamonds) and the tapered waist (red squares), is shown in Fig. 4(a). The as-drawn fiber is clearly made up of several millimeter long crystal grains, some of which overlap, in agreement with previous measurements of these fibers [8, 14]. However, the tapered region is found to consist of only a single grain which extends over a length of  $\sim 9$  mm, verifying that the crystallinity has been improved by the tapering process, as predicted in [4]. Moreover, to assess the single crystallinity across the whole cross-section, the fiber was rotated around its axis to verify no other crystals were present.

Additional measurements were also conducted on two further tapered fibers with waist diameters of  $3\ \mu\text{m}$  and  $0.9\ \mu\text{m}$ , with the longest measured single crystal grain in each fiber reported in Fig. 4(d). This table shows a general trend of increasing grain size for decreasing core size, in the micrometer range, which we attribute to faster cooling rates that help to suppress the number of nucleation sites to enable the formation of larger grains [14–16]. We note that the slightly smaller grain size measured for the sub-micron core fiber is most likely due to the fact that the CaO interface layer is not optimized for these dimensions, resulting in an increased strain between the core and cladding materials, and this is something that we will address in future work. Nevertheless, we expect the increased grain sizes measured in the tapered fibers to significantly improve the transmission properties of the polysilicon fibers, as by reducing the number of grain boundaries we also reduce the defect material that surrounds these. Evidence for this is provided by the values for the optical losses reported in Fig. 4 (d), which were measured using the cut-back method at the telecoms wavelength of  $1.55\ \mu\text{m}$ . To ensure consistency in the measurements, these values were obtained by repeatedly polishing off 1 mm segments within the uniform waist section of the fiber, which had a typical length of  $\sim 1$  cm. Thus these values represent an average loss of the fundamental mode through the tapered waist of the fiber. Significantly, the losses of  $\sim 2$  dB/cm reported for the  $1\text{--}2\ \mu\text{m}$  diameter fibers represent a marked improvement (of more than 1 dB/cm) over our previous results in [4]. Thus we expect that comprehensive XRD characterizations could be used to further optimize the tapering process to produce even longer single crystal grains in both the micro and nano-scale cores, ultimately allowing for the production of silicon fibers with losses of  $< 1$  dB/cm.



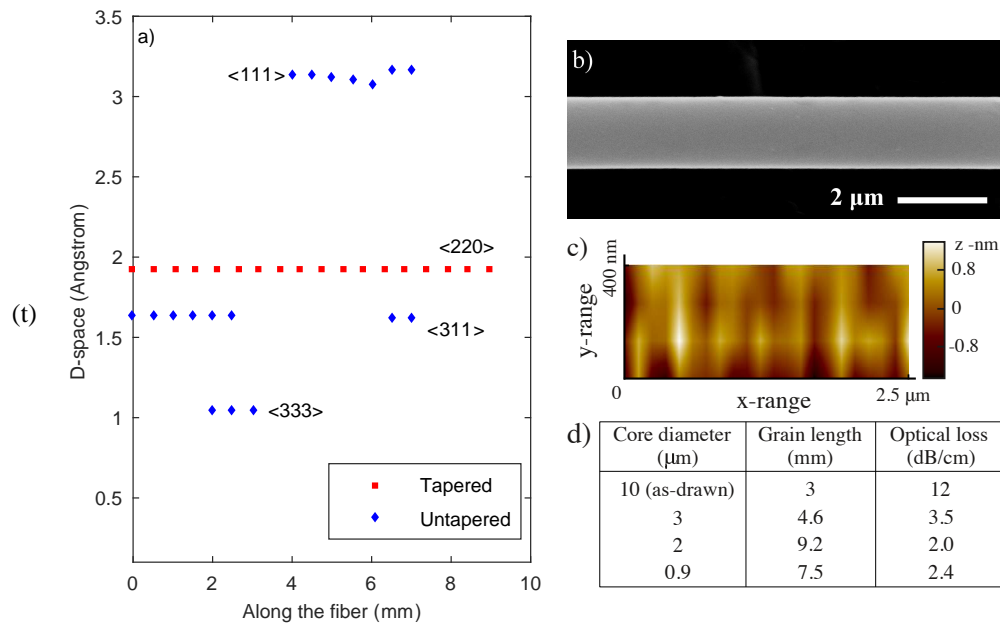


Fig. 4. a) Lattice spacing of diffraction spots measured via XRD along the as-drawn fiber (blue) and a tapered waist (red), corresponding to the labeled crystallographic planes. b) SEM and c) topographical ZeScope image of an etched silicon fiber waist. d) Measurements of the maximum grain length together with loss values for different tapered waists.

## 5. Core/cladding interface quality

Although we expect that for the micron-sized fibers used in this work the main source of loss will be from the bulk material, as we continue to scale the core sizes down towards the nanoscale regime, the surface quality of the silicon/silica interface will play an increasingly important role. As a final investigation, we have used a buffered hydrofluoric acid solution to etch the silica cladding away from the core, so that we can assess the surface roughness of the silicon wire directly. Fig. 4(b) shows a SEM image of an etched section of the tapered waist, revealing a smooth surface without any obvious grain boundaries. Further confirmation of the good interface quality was obtained using a ZeScope three dimensional optical profiler, from which we measured a root-mean-square roughness of  $\sim 0.7$  nm, as shown in Fig. 4(c). Thus, these results confirm the tapering procedure as a viable route to obtaining low loss crystalline silicon fibers with sub-micron core sizes, which would be of great value for nonlinear applications [17].

## 6. Conclusion

We have reported a crystallographic study of the core materials in tapered silicon optical fibers. The results confirm that the lower losses measured for the fibers after tapering are due to the large single crystal grains that form in the micron-sized tapered waists as the material recrystallizes. Although the tapering procedure does introduce a small amount of strain into the reduced cores, this is not sufficient to alter the transmission properties [18], as confirmed via the low measured optical losses. We believe that the tapering approach could be applied to other semiconductor core fibers as a way to improve the crystallinity and to reach core diameters desired for many optical applications [5, 9].

## Funding

EPSRC (EP/J004863/1 and EP/P000940/1); NORFAB; and the Norwegian Discovery Fund.

## Acknowledgments

We thank Fariza H. Suhailin for help with the preliminary tapering work and the Diamond Light Source for access to the I18 beamline (SP13025). The data for this paper are accessible through the University of Southampton Institutional Research Repository (DOI:10.5258/SOTON/D0015).